



Comparative studies of efficiency droop in polar and non-polar InGaN quantum wells

M. J. Davies, P. Dawson, S. Hammersley, T. Zhu, M. J. Kappers, C. J. Humphreys, and R. A. Oliver

Citation: [Applied Physics Letters](#) **108**, 252101 (2016); doi: 10.1063/1.4954236

View online: <http://dx.doi.org/10.1063/1.4954236>

View Table of Contents: <http://scitation.aip.org/content/aip/journal/apl/108/25?ver=pdfcov>

Published by the [AIP Publishing](#)

Articles you may be interested in

[The microstructure of non-polar a-plane \(112 \$\bar{0}\$ \) InGaN quantum wells](#)

J. Appl. Phys. **119**, 175703 (2016); 10.1063/1.4948299

[Temperature-dependent efficiency droop of blue InGaN micro-light emitting diodes](#)

Appl. Phys. Lett. **105**, 171107 (2014); 10.1063/1.4900865

[Identification of nnp and npp Auger recombination as significant contributor to the efficiency droop in \(GaIn\)N quantum wells by visualization of hot carriers in photoluminescence](#)

Appl. Phys. Lett. **103**, 071108 (2013); 10.1063/1.4818761

[High excitation carrier density recombination dynamics of InGaN/GaN quantum well structures: Possible relevance to efficiency droop](#)

Appl. Phys. Lett. **102**, 022106 (2013); 10.1063/1.4781398

[The consequences of high injected carrier densities on carrier localization and efficiency droop in InGaN/GaN quantum well structures](#)

J. Appl. Phys. **111**, 083512 (2012); 10.1063/1.3703062



NEW Special Topic Sections

NOW ONLINE
Lithium Niobate Properties and Applications:
Reviews of Emerging Trends

AIP Applied Physics Reviews

The banner features a blue background with a glowing light effect on the right. On the left, there is a small image of an Applied Physics Reviews journal cover showing a technical diagram. The text is in white and yellow, with the AIP logo in white.

Comparative studies of efficiency droop in polar and non-polar InGaN quantum wells

M. J. Davies,¹ P. Dawson,¹ S. Hammersley,¹ T. Zhu,² M. J. Kappers,² C. J. Humphreys,² and R. A. Oliver²

¹*School of Physics and Astronomy, Photon Science Institute, University of Manchester, M13 9PL Manchester, United Kingdom*

²*Department of Material Science and Metallurgy, 27 Charles Babbage Road, University of Cambridge, Cambridge CB3 0FS, United Kingdom*

(Received 21 March 2016; accepted 7 June 2016; published online 20 June 2016)

We report on a comparative study of efficiency droop in polar and non-polar InGaN quantum well structures at $T = 10$ K. To ensure that the experiments were carried out with identical carrier densities for any particular excitation power density, we used laser pulses of duration ~ 100 fs at a repetition rate of 400 kHz. For both types of structures, efficiency droop was observed to occur for carrier densities of above $7 \times 10^{11} \text{ cm}^{-2} \text{ pulse}^{-1}$ per quantum well; also both structures exhibited similar spectral broadening in the droop regime. These results show that efficiency droop is intrinsic in InGaN quantum wells, whether polar or non-polar, and is a function, specifically, of carrier density. © 2016 Author(s). All article content, except where otherwise noted, is licensed under a Creative Commons Attribution (CC BY) license (<http://creativecommons.org/licenses/by/4.0/>).
<http://dx.doi.org/10.1063/1.4954236>

InGaN/GaN quantum well (QW) structures grown along the polar c direction are subject to very large macroscopic electric fields due to the piezoelectric and spontaneous polarisations inherent to this type of structure. These electric fields can be eliminated if the QWs are grown on non-polar planes.¹ Initially, it was suggested that the main advantage of non-polar InGaN/GaN QWs over their polar counterparts would be enhanced recombination efficiency due to the much shorter radiative lifetimes^{2,3} compared to equivalent c -plane structures.^{4–8} Recently, it has also been suggested that the phenomena of efficiency droop could also be influenced by the polarity of the QW structure. Efficiency droop, the reduction in the efficiency of light emitting diodes at high drive currents, is one of the most serious problems in the use of nitride Light emitting diodes (LEDs) for high brightness applications.^{9,10} Several mechanisms have been put forward to explain droop, including problems with hole injection,^{10,11} Auger recombination,^{12,13} carrier escape,¹⁴ and non-radiative recombination following the saturation of localised states.^{15–17} There are now a number of publications suggesting that non-polar InGaN QWs may be less susceptible to efficiency droop than c -plane structures and a range of explanations have been put forward to explain these observations. Several groups have linked this behaviour directly to the absence of the internal electric fields. From measurements on non-polar LEDs, Ling *et al.*¹⁸ and Li *et al.*¹⁹ assigned the reduction in droop to reduced losses associated with carrier spill over due to the improved carrier confinement. However, an alternative explanation was put forward by Li *et al.*²⁰ and Chang *et al.*²¹ who suggested that droop was reduced because of the improvement in hole distribution amongst the QWs in multiple QW LEDs. Also in the theoretical treatment by Vaxenburg *et al.*,²² it was suggested that for GaN/AlN QWs the rate of Auger recombination is directly influenced by the polarisation fields and hence Auger, which is widely

believed^{12,23–25} to be responsible for efficiency droop, would have less effect in non-polar structures. A different form of explanation has been put forward by Kioupakis *et al.*^{26,27} linking the reduction in polarisation field to an increase in both the radiative recombination and non-radiative recombination rates such that the improved droop behaviour in non-polar QWs is not due not to an improvement in the competition between radiative and non-radiative recombination paths, but rather a reduction in the operating carrier density at a given current density. Such behaviour has been reported²⁸ experimentally for semi-polar QW LEDs.

To throw further light on this question, we have studied the photoluminescence (PL) efficiency and recombination dynamics of m -plane (non-polar) and c -plane (polar) InGaN/GaN QW structures, as a function of photo-excited carrier density at 10 K. In particular, we have used short pulse laser excitation (pulse width 100 fs) where the repetition rate greatly exceeds the inverse of the recombination time so that the peak carrier density is determined solely by the excitation power density. This removes the problem that arises in CW photoluminescence (PL) and electroluminescence (EL) experiments that under steady-state excitation conditions the equilibrium carrier densities in c -plane and m -plane structures can be very different due to the dependence on the different recombination rates. The importance of the role of the recombination rate in determining droop, hence excited carrier density, has already been shown by David *et al.*²⁹ for polar InGaN LEDs with varying In fraction. In this work, it was shown that decreases in the recombination rate as the In fraction increased lead to the occurrence of efficiency droop at progressively lower current densities.

Two InGaN/GaN QW InGaN/GaN structures were studied: both grown by metal-organic vapour phase epitaxy. The non-polar sample was grown on an m -plane free standing GaN substrate [Ammono SA], with 2° miscut toward the (000-1) axis using the quasi 2 temperature growth technique.^{30,31} The



substrate had a negligible basal-plane stacking fault density and a threading dislocation density of $<10^5 \text{ cm}^{-2}$. The QW structure consisted of 5 periods of $2.4 \pm 0.3 \text{ nm}$ InGaN wells with an In fraction of 0.28 and GaN barriers of thickness $6.1 \pm 0.3 \text{ nm}$. In particular, we note that the final GaN barrier layer acts as the capping layer. Comprehensive details of the quasi-two temperature³⁰ growth schedule and structural details of this sample can be found elsewhere.³² The polar sample is a *c*-plane InGaN/GaN single QW structure grown on a (0001) sapphire substrate with an In fraction of 0.15 and a thickness of 2.9 nm at a temperature of 750°C using a single temperature growth methodology.³³ The structural properties of the *c*-plane sample are further described in Ref. 33. In particular, we note that the thickness of the GaN cap layer was 7 nm . These samples were chosen as they both had a low temperature emission peak energy of $\sim 2.660 \text{ eV}$. The optical properties were studied using a combination of time-integrated PL spectroscopy and PL decay time measurements. The samples were mounted on the cold finger of a temperature controlled closed-cycle helium cryostat. The samples were excited using the frequency tripled output of a 100 fs mode locked Ti:sapphire laser, with a photon energy of 4.881 eV . The use of a pulsed laser, with a pulse duration much shorter than the carrier recombination lifetimes for both samples,^{2,8,34} ensures that the peak carrier concentration in the QWs is determined by the power density of the excitation source. This assumes that the light is mainly absorbed due to the excitation of carriers in the GaN and that these carriers are captured by the QWs. Time integrated PL spectroscopy was performed by modulating the laser light with a chopper and by dispersing the PL through a 0.75 m single grating spectrometer which was then detected by a GaAs photomultiplier tube, the signal from the photomultiplier was then processed by a lock-in detector. For the PL time decay measurements, a micro-channel plate detector was used to detect the PL via the spectrometer and the signal was processed using the technique of time-correlated single photon counting.

The emission spectra at low temperature for the *m*-plane and *c*-plane samples taken under conditions of low CW excitation power density have previously been shown in Refs. 31 and 32, respectively. The PL spectrum from the *m*-plane sample consists of a broad emission band with peak energy of 2.615 eV and full width at half maximum height (FWHM) of 158 meV . The spectrum of the *c*-plane sample consists of a main peak whose peak energy is 2.669 eV with a FWHM of 75 meV along with several LO phonon replicas³² at lower energy. For both samples, as shown in Figure 1(b), the PL FWHM remains constant within the experimental error at 158 meV and 75 meV for the non-polar and polar samples, respectively, up to a value of peak carrier density per pulse per QW equal to 1×10^{12} . The large spectral line widths of both the *m*- and *c*-plane structures at low excitation are attributed to the effects of exciton or carrier localisation, respectively, at random fluctuations in the In fraction of the InGaN QWs.^{33,35,36}

Plots of the integrated PL intensity per unit excitation power (I_{PL}) versus peak carrier density per pulse per QW at 10 K for the two samples are shown in Figure 1(a). For the lower values of excitation carrier density, I_{PL} is constant, reflecting the assumption that the internal quantum efficiency is 100% at 10 K . Thus, on this basis, the maximum value of I_{PL} is set to 1. Also, the data on the *x* axis is plotted as a

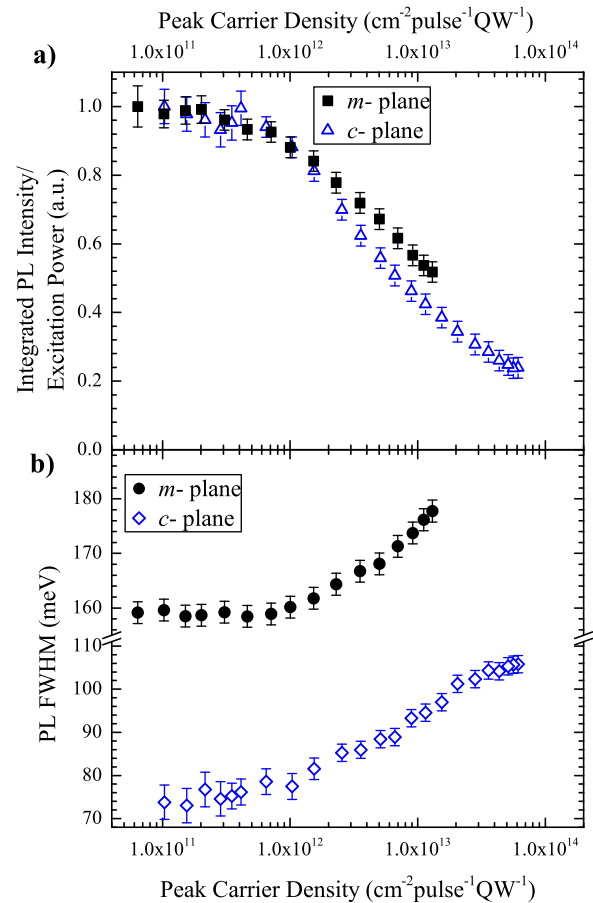


FIG. 1. (a) Integrated PL intensity as a function of peak carrier density of the *m*-plane and *c*-plane samples, measured at 10 K , as a function of peak carrier density. (b) FWHM of the PL spectra as a function of peak carrier density.

function of peak carrier density per pulse per QW ($\text{cm}^{-2}\text{pulse}^{-1}\text{QW}^{-1}$). Specifically, the “per QW” aspect is included to try to account for the different numbers of QWs in the different samples. For the excitation photon energy of 4.881 eV , the majority of carriers are excited in the GaN layers. We assume that all the carriers are captured by the QW(s); this assumption is supported by the fact that we do not observe a significant amount of recombination from the various GaN layers in the samples. Also, we assume that in the non-polar sample the carriers are evenly distributed amongst the 5 QWs. Therefore, the peak carrier densities per pulse (also indicated in Figure 1) in the QWs of non-polar sample is expected to be one fifth of the maximum peak carrier density generated in the single QW. As can be seen in Figure 1(a), the values of I_{PL} for both the *m*-plane and *c*-plane samples roll off at around same injected peak carrier density of $7 \times 10^{11} \text{ cm}^{-2}\text{pulse}^{-1}\text{QW}^{-1}$. Thus, efficiency droop is observed for both the *c*-plane and *m*-plane structures at the same peak carrier density.

The similarity in the values of peak carrier density required to produce the onset of efficiency droop is not the only common feature in the behaviour of the *m*-plane and *c*-plane structures. In Figure 1(b), the PL FWHM of both samples is shown, as a function of peak carrier density per pulse per QW at 10 K . For both samples, the PL FWHM remains constant at 158 meV and 75 meV for the non-polar

and polar samples, respectively, up to a value of peak carrier density per pulse per QW equal to 1×10^{12} . As the peak carrier density per pulse per QW was increased beyond this figure, the PL FWHM also increased up to the values of 178 meV for non-polar sample and 106 meV for the polar sample. The behaviour of the *c*-plane spectra is similar to that reported previously in the work by Brosseau *et al.*,³⁷ Sun *et al.*,³⁸ and Davies *et al.*³⁹ In particular, in the work of Davies *et al.*, the increase in PL FWHM was correlated with the onset of droop and was interpreted as being due to an extra emission component involving delocalised carriers.

In Figure 2, PL spectra for the *m*-plane sample are shown, which are representative of those measured below and above the peak carrier densities required to produce efficiency droop, namely, $10^{11} \text{ cm}^{-2} \text{ pulse}^{-1} \text{ QW}^{-1}$ and $1.4 \times 10^{13} \text{ cm}^{-2} \text{ pulse}^{-1} \text{ QW}^{-1}$. A clear increase in the FWHM of the spectrum is apparent at the highest excitation carrier density and occurs because of the emergence of a tail on the high energy side of the spectrum. To investigate further the emergence of the high energy tail, PL decay transients were measured across the PL spectrum at excitation carrier densities both above and below the onset of efficiency droop. In all cases, the decay curves were single exponential and could be characterised by a single decay constant. In Figure 2, the measured decay constants across the PL spectrum of the non-polar sample are shown, measured with an excitation power density below the threshold carrier density for efficiency droop and with the highest carrier density possible (see Figure 1(a)). In the case of the low excitation density measurements, the decay constant was largely independent of detection energy and had a value of 260 ± 15 ps. This behaviour is consistent with the initial work of Marcinkevicius *et al.*² and our previous measurements.³³ In all the previous work, the decay constants were assigned to be governed by radiative processes only so the similarity between our values of the decay constant and the work of others adds weight to our assumption that under the low injection conditions the efficiency of radiative recombination is 100%. Under the low power excitation conditions,

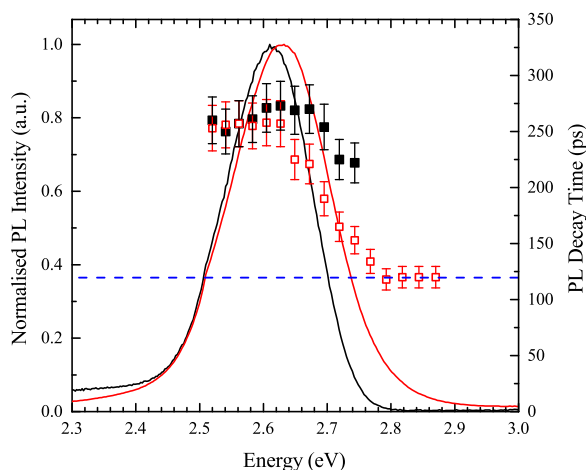


FIG. 2. Time-integrated PL spectra for the *m*-plane sample along with PL decay times measured across the PL spectrum for peak carrier excitation densities of $10^{11} \text{ cm}^{-2} \text{ pulse}^{-1} \text{ QW}^{-1}$ (black line and black data points) and $1.4 \times 10^{13} \text{ cm}^{-2} \text{ pulse}^{-1} \text{ QW}^{-1}$ (red line and red data points), i.e., measured below and above the onset of efficiency droop. The blue dashed line indicates the instrumental time response.

we note a small drop in the decay constant to a value of 225 ± 15 ps on the high energy side of the spectrum. The origin of this reduction is currently unclear but we suggest that it may be due to the effects of carrier hopping to deeper localised states as has been observed previously in other localised systems.^{40–42}

For the high carrier density, we note a distinct change in recombination dynamics on the high energy side of the spectrum, at energies associated with the tail which appears at high carrier density. For the majority of the spectrum, the decay constants remain unchanged at 260 ± 15 ps. However, on the high energy side of the spectrum, when the decay transients are measured at energies above 2.6 eV, the decay constants drop rapidly from 260 ± 15 ps to 120 ± 15 ps, the lowest values of 120 ps being limited by the instrumental response. The fact the decay constants associated with the main emission band are unchanged at high excitation power densities suggests that the recombination responsible for the main emission band remains purely radiative at the highest carrier densities. This suggests that the new recombination channel on the high energy side of the spectrum is affected by non radiative processes that could be responsible for the short decay constant.

This overall behaviour of the *m*-plane sample is very similar to that reported previously³⁸ for the *c*-plane sample. In this previous work, in the droop regime at the highest excitation carrier densities, a second emission band emerged on the high energy side of the PL spectrum. This band is responsible for the increases in the FWHM of the spectrum of the *c*-plane sample shown in Figure 1(b). The second emission band had a much shorter decay time and was attributed to the recombination of weakly localised or delocalised carriers that occurs due to the saturation of the localised states. Efficiency droop in *c*-plane QWs at low temperatures has also been shown previously³⁹ to correlate with the saturation of localised states, in particular, those responsible for the localisation of holes¹⁶ leading to the proposal^{16,43,44} that saturation of the localised states is a key precursor to the non-radiative losses responsible for efficiency droop. This behaviour is broadly in line with the original suggestion by Hader *et al.*¹⁵

In summary, we have shown that, most importantly, efficiency droop does occur in non-polar QWs as long as the injected carrier density is sufficiently large. Indeed, as long as the recombination time does not influence the carrier density then, based on the assumption that the QWs are equally populated, the critical carrier density for the onset of droop is remarkably similar for both the polar and non-polar structures. Also, not only are the critical carrier densities the same, but in both polar and non-polar structures we observe the same signature associated with droop in the PL spectra, i.e., a broadening on the high energy side of the spectra. Following on from our previous work,³⁹ we attribute the broadening of the spectra to recombination associated with delocalised carriers, of which a significant proportion recombines non-radiatively. These observations suggest that there is a common mechanism responsible for the efficiency droop, in which delocalised carriers recombine non-radiatively. Our data do not reveal the nature of the non-radiative recombination mechanism, although either Auger recombination or Shockley-Read-Hall

recombination at defects is a plausible candidate. However, it would appear that the efficiency droop is an intrinsic effect that is determined by the carrier density in both polar and non-polar InGaN QWs. We note, in particular, that this final statement would be true even without the assumption that the QWs are equally populated in the *m*-plane sample.

This work was carried out with the support of the United Kingdom Engineering and Physical Sciences Research Council under Grant Nos. EPJ001627\1 and EPJ003603\1. The data associated with the paper are openly available from the University of Manchester eScholar Data Repository: <http://dx.doi.org/10.15127/1.301529>.

- ¹P. Waltereit, O. Brandt, A. Trampert, H. T. Grahn, J. Menniger, M. Ramsteiner, M. Reiche, and K. H. Ploog, *Nature* **406**, 865 (2000).
- ²S. Marcinkevicius, K. M. Kelchner, L. Y. Kuritzky, S. Nakamura, S. P. DenBaars, and J. S. Speck, *Appl. Phys. Lett.* **103**, 111107 (2013).
- ³G. A. Garrett, H. Shen, M. Wraback, A. Tyagi, M. C. Schmidt, J. S. Speck, S. P. DenBaars, and S. Nakamura, *Phys. Status Solidi C* **6**, S800 (2009).
- ⁴T. Akasaka, H. Gotoh, H. Nakano, and T. Makimoto, *Appl. Phys. Lett.* **86**, 191902 (2005).
- ⁵O. Mayrock, H.-J. Wunsche, and F. Henneberger, *Phys. Rev. B* **62**, 16870 (2000).
- ⁶S. F. Chichibu, T. Azuhata, T. Sota, T. Mukai, and S. Nakamura, *J. Appl. Phys.* **88**, 5153 (2000).
- ⁷J. Wang, L. Wang, W. Zhao, Z. Hao, and Y. Luo, *Appl. Phys. Lett.* **97**, 201112 (2010).
- ⁸J. A. Davidson, P. Dawson, T. Wang, T. Sugahara, J. W. Orton, and S. Sakai, *Semicond. Sci. Technol.* **15**, 497 (2000).
- ⁹H. Morkoc, *Handbook of Nitride Semiconductors and Devices* (Wiley VCH, Berlin, 2008), Vol. 3.
- ¹⁰J. Xie, X. Ni, Q. Fan, R. Shimada, U. Ozgur, and H. Morkoc, *Appl. Phys. Lett.* **93**, 121107 (2008).
- ¹¹I. A. Pope, P. M. Smowton, P. Blood, J. D. Thompson, M. J. Kappers, and C. J. Humphreys, *Appl. Phys. Lett.* **82**, 2755 (2003).
- ¹²N. F. Gardner, G. O. Muller, Y. C. Shen, G. Chen, S. Watanabe, W. Gotz, and M. R. Krames, *Appl. Phys. Lett.* **91**, 243506 (2007).
- ¹³J. Iveland, L. Martinelli, J. Peretti, J. S. Speck, and C. Weisbuch, *Phys. Rev. Lett.* **110**, 177406 (2013).
- ¹⁴M. Schubert, J. Xu, Q. Dai, F. W. Mont, K. J. Kim, and E. F. Schubert, *Appl. Phys. Lett.* **94**, 081114 (2009).
- ¹⁵J. Hader, J. V. Moloney, and S. W. Koch, *Appl. Phys. Lett.* **96**, 221106 (2010).
- ¹⁶S. Hammersley, D. Watson-Parris, P. Dawson, T. J. Godfrey, M. J. Kappers, C. McAleese, R. A. Oliver, and C. J. Humphreys, *J. Appl. Phys.* **111**, 083512 (2012).
- ¹⁷G. Pozina, R. Ciechonski, Z. Bi, L. Samulson, and B. Monemar, *Appl. Phys. Lett.* **107**, 251106 (2015).
- ¹⁸S.-C. Ling, T.-C. Lu, S.-P. Chang, J.-R. Chen, J.-R. Kuo, and S.-C. Wang, *Appl. Phys. Lett.* **96**, 231101 (2010).
- ¹⁹X. Li, X. Ni, H. Y. Liu, F. Zhang, S. Liu, J. Lee, V. Avrutin, U. Ozgur, T. Paskova, G. Mulholland, K. R. Evans, and H. Morkoc, *Phys. Status Solidi C* **8**, 1560 (2011).
- ²⁰X. Li, X. Ni, J. Lee, M. Wu, U. Ozgur, H. Morkoc, T. Pakova, G. Mulholland, and K. R. Evans, *Appl. Phys. Lett.* **95**, 121107 (2009).
- ²¹S.-P. Chang, T.-C. Lu, L.-F. Zhuo, C.-Y. Jang, D.-W. Lin, H.-C. Yang, H.-C. Kuo, and S.-C. Wang, *J. Electrochem. Soc.* **157**, H501 (2010).
- ²²R. Vaxenburg, A. Rodina, E. Lifshitz, and A. L. Efros, *Appl. Phys. Lett.* **103**, 221111 (2013).
- ²³Y. C. Shen, G. O. Mueller, S. Watanabe, N. F. Gardner, A. Munkholm, and M. R. Krames, *Appl. Phys. Lett.* **91**, 141101 (2007).
- ²⁴J. Iveland, M. Piccardo, L. Martinelli, J. Peretti, J. W. Choi, N. Young, S. Nakamura, J. S. Speck, and C. Weisbuch, *Appl. Phys. Lett.* **105**, 052103 (2014).
- ²⁵M. Binder, A. Nirschl, R. Zeisel, T. Hager, H.-J. Lugauer, M. Sabathil, D. Bougeard, J. Wagner, and B. Galler, *Appl. Phys. Lett.* **103**, 071108 (2013).
- ²⁶E. Kioupakis, Q. Yan, and C. G. Van de Walle, *Appl. Phys. Lett.* **101**, 231107 (2012).
- ²⁷E. Kioupakis, Q. Yan, D. Steiauf, and C. G. Van de Walle, *New J. Phys.* **15**, 125006 (2013).
- ²⁸C. C. Pan, S. Tanaka, F. Wu, F. Zhao, J. S. Speck, S. Nakamura, S. P. DenBaars, and D. Feezel, *Appl. Phys. Express* **5**, 062103 (2012).
- ²⁹A. David and M. J. Grundmann, *Appl. Phys. Lett.* **97**, 033501 (2010).
- ³⁰S. J. Leem, Y. C. Shin, E. H. Kim, C. M. Kim, B. G. Lee, Y. Moon, I. H. Lee, and T. G. Kim, *Semicond. Sci. Technol.* **23**, 125039 (2008).
- ³¹R. A. Oliver, F. C.-P. Massabau, M. J. Kappers, W. A. Phillips, E. J. Thrush, C. C. Tartan, W. E. Blenkhorn, T. J. Badcock, P. Dawson, M. A. Hopkins, C. C. Humphreys, D. W. Allsopp, and C. J. Humphreys, *Appl. Phys. Lett.* **103**, 141114 (2013).
- ³²D. Sutherland, T. Zhu, J. T. Griffiths, F. Tang, P. Dawson, D. Kundys, F. Oehler, M. J. Kappers, C. J. Humphreys, and R. A. Oliver, *Phys. Status Solidi B* **252**, 965 (2015).
- ³³D. M. Graham, A. Soltani-Vala, P. Dawson, M. J. Godfrey, T. M. Smeeton, J. S. Barnard, M. J. Kappers, C. J. Humphreys, and T. J. Thrush, *J. Appl. Phys.* **97**, 103508 (2005).
- ³⁴S. Schulz, D. P. Tanner, E. P. O'Reilly, M. A. Caro, T. L. Martin, P. A. J. Bagot, M. P. Moody, F. Tang, J. T. Griffiths, F. Oehler, M. J. Kappers, R. A. Oliver, C. J. Humphreys, D. Sutherland, M. J. Davies, and P. Dawson, *Phys. Rev. B* **92**, 235419 (2015).
- ³⁵D. Watson-Parris, M. J. Godfrey, P. Dawson, R. A. Oliver, M. J. Galtrey, M. J. Kappers, and C. J. Humphreys, *Phys. Rev. B* **83**, 115321 (2011).
- ³⁶S. Schulz, M. A. Caro, C. Coughlan, and E. P. O'Reilly, *Phys. Rev. B* **91**, 035439 (2015).
- ³⁷C. N. Brosseau, M. Perrin, C. Silva, and R. Leonelli, *Phys. Rev. B* **82**, 085305 (2010).
- ³⁸G. Sun, G. Xu, Y. J. Ding, H. Zhao, G. Liu, J. Zhang, and N. Tansu, *Appl. Phys. Lett.* **99**, 081104 (2011).
- ³⁹M. J. Davies, T. J. Badcock, P. Dawson, M. J. Kappers, R. A. Oliver, and C. J. Humphreys, *Appl. Phys. Lett.* **102**, 022106 (2013).
- ⁴⁰G. Gourdon and P. Lavallard, *Phys. Status Solidi B* **153**, 641 (1989).
- ⁴¹H. Kalt, J. Collet, S. D. Baranowski, R. Saleh, P. Thomas, L. S. Dang, and J. Cibert, *Phys. Rev. B* **45**, 4253 (1992).
- ⁴²O. Rubel, W. Stolz, and S. D. Baranowski, *Appl. Phys. Lett.* **91**, 021903 (2007).
- ⁴³N. I. Bochkareva, Y. T. Rebane, and Y. G. Scheter, *Appl. Phys. Lett.* **103**, 191101 (2013).
- ⁴⁴R. Aleksiejunas, K. Gelzinyte, S. Nargelas, K. Jarasiunas, M. Vengris, E. A. Armour, D. P. Byrnes, R. A. Arif, S. M. Lee, and G. D. Papanoulitis, *Appl. Phys. Lett.* **104**, 022114 (2014).